Results in Physics 9 (2018) 1172–1184

Contents lists available at ScienceDirect

Results in Physics

journal homepage: www.elsevier.com/locate/rinp

Influence of wall couple stress in MHD flow of a micropolar fluid in a porous medium with energy and concentration transfer

Asma Khalid[b], Ilyas Khan[a,*], Arshad Khan[c], Sharidan Shafie[d]

[a] Faculty of Mathematics and Statistics, Ton Duc Thang University, Ho Chi Minh City, Viet Nam
[b] Department of Mathematics, Sardar Bahadur Khan Women's University, Quetta 87300, Pakistan
[c] Institute of Business and Management Sciences, The University of Agriculture, Peshawar, KPK, Pakistan
[d] Department of Mathematical Sciences, Faculty of Science, Universiti Teknologi Malaysia, 81310 UTM Skudai, Malaysia

ARTICLE INFO

Keywords:
Micropolor fluid
Microrotation
MHD
Porosity
Wall couple stress
Exact solutions

ABSTRACT

The intention here is to investigate the effects of wall couple stress with energy and concentration transfer in magnetohydrodynamic (MHD) flow of a micropolar fluid embedded in a porous medium. The mathematical model contains the set of linear conservation forms of partial differential equations. Laplace transforms and convolution technique are used for computation of exact solutions of velocity, microrotations, temperature and concentration equations. Numerical values of skin friction, couple wall stress, Nusselt and Sherwood numbers are also computed. Characteristics for the significant variables on the physical quantities are graphically discussed. Comparison with previously published work in limiting sense shows an excellent agreement.

Introduction

The theory of micropolar has received enormous attentions during the recent years since the traditional Newtonian fluids cannot specifically depict the feature of fluid with suspended particles, polar fluids, suspension solutions, liquid crystals, colloidal solutions and fluid containing small additives. Physically, micropolar fluids may present the non-Newtonian fluids consisting of short rigid cylindrical elements or dumb-bell molecules, polymer fluids, fluids suspensions and animal blood. The existence of dust or smoke particular in a gas may also be modeled using micropolar fluid dynamics. Eringen [1] first derived the theory of micropolar fluids, which illustrates the microrotation effects to the microstructures. Eringen [2] extended his idea to the theory of thermomicropolar fluids, which interest to the special effects of microstructures on the fluid flow. The mathematical theory of equations of micropolar fluids and applications of these fluids in the theory of lubrication and in the theory of porous media are given in recent books by Eringen [3] and Lukaszewicz [4].

Combined heat and mass transfer phenomena have great significance in engineering and industrial applications in drying, evaporation at the surface of a water body, energy transfer in a wet cooling tower, polymer productions, food processing, the flow in a desert cooler, and geothermal system; therefore this area of research received an extensive attention in recent years [5–7]. The study of magnetohydrodynamic (MHD) flow has received an immense interest due to its importance in many engineering applications such as, liquid metals system of fusion reactors, plasma studies, petroleum industries, cooling of nuclear reactors, MHD power generators, crystal growth and the boundary layer control in aerodynamics [8–12]. The micropolar fluids problems through porous media have many applications, such as porous rocks, foams and foamed solids, alloys, polymer blends, aerogels, and microemulsions. In recent years, many researchers have discussed unsteady free convection flow of a micropolar fluid with and without a magnetic field through a porous medium for example [13–17].

Agarwal et al. [18] discussed heat transfer in micropolor fluid past a porous stationary wall. Srinivasacharya and Rajyalakshmi [19] illustrated the problem of creeping flow of a micropolar fluid past a porous sphere. Abo-Eldahab and Ghonaim [20] presented the radiation effect on heat transfer of a micropolar fluid through a porous medium. Damesh et al. [21] reported the micropolar fluid with unsteady natural convection heat transfer over a vertical surface with constant heat flux using numerical technique. Nadeem et al. [22] analyzed the MHD stagnation flow of a micropolar fluid through a porous medium. Aurangzaib et al. [23] examined the unsteady MHD mixed convection flow of micropolar fluid with heat and mass transfer over a vertical plate in a porous medium. Modatheri et al. [24] studied the oscillatory flow of a micropolar fluid over a vertical permeable plate in a porous medium with MHD effects. Mostafa et al. [25] investigated the MHD flow and heat transfer of a micropolar fluid with slip velocity over a stretching

* Corresponding author.
E-mail address: ilyaskhan@tdt.edu.vn (I. Khan).

https://doi.org/10.1016/j.rinp.2018.04.005
Received 20 November 2017; Received in revised form 2 April 2018; Accepted 5 April 2018
Available online 19 April 2018

surface with heat generation (absorption). Haque et al. [26] presented the micropolar fluid behaviour on steady MHD free convection and mass transfer flow with constant heat and mass fluxes, joule heating and viscous dissipation.

Abo-Dahab and Mohamed [27] reported the unsteady flow of rotating and chemically reacting MHD micropolar fluid in slip-flow regime with heat generation. Influence of heat with source or sink on MHD flow of micropolar fluids over a shrinking sheet with mass suction has been discussed by Sajjad and Farooq [28]. Mishra et al. [29] studied MHD free convection flow of a micropolar fluid with heat source. Analytic solution for heat and mass transfer problem of a micropolar fluid in a porous channel by using Differential Transformation Method (DTM) was carried out by Sheikholeslami et al. [30]. Hussanan et al. [31] examined the effects of chemical reaction and thermal radiation on unsteady free convection flow of micropolar fluid with Newtonian heating. Unsteady free convection flow of a micropolar fluid past a semi-infinite vertical plate embedded in a porous medium in the presence of heat absorption with Newtonian heating was investigated by Baker et al. [32]. Khalid et al. [33] presented the exact solutions of conjugate transfer of heat and mass in unsteady flow of a micropolar fluid with wall couple stress. Mohanty et al. [34] illustrated heat and mass transfer effect of micropolar fluid over a stretching sheet through porous media numerically whereas Pal and Biswas [35] studied MHD oscillatory flow on convective-radiative heat and mass transfer of micropolar fluid in a porous medium with chemical reaction by using perturbation technique.

The couple stress fluids are proficient of describing different types of lubricants, suspension fluids, blood, etc. Moreover, some of the non-Newtonian flow characteristics of blood can be explained by supposing the blood to be a fluid with couple stress. It is well recognized that at low shear stress rates during its flow through narrow vessels, being the suspension of cells, blood behave like a non-Newtonian fluid [36]. Ramanaiah discussed Squeeze films between finite plates lubricated by fluids with couple stresses [37]. Mokhiamar et al. [38] studied journal bearing lubricated by fluid with couple stresses. Zakaria [39] analyzed the unsteady free convection of couple stress fluid through a porous medium. Sreenadh et al. [40] examined the influence of MHD on the couple stress fluid in the porous medium. Khan and Riaz [41] studied the three dimensional flow of couple stress fluid over a rotating disk. Rani et al. [42] investigated the couple stress fluid over an infinite vertical cylinder. Effects of Hall and ion-slip on couple stress fluid between the parallel disks are presented by Sirnivasacharya et al. [43]. El-Dabe and El-Mohandis [44] discussed the effect of couple stress on pulsatile hydromagnetic Poiseuille flow. Farooq et al. [45] examined the laminar flow of couple stress fluids for Vogel's model. Khan et al. [46] obtained the approximate solution of couple stress fluid with expanding or contracting porous channel.

To the best of author's knowledge so far, no study has been conducted to investigate the energy and concentration phenomenon in MHD flow of a micropolar fluid over an oscillating vertical plate embedded in a porous medium, especially when exact solutions are required. The Laplace transforms technique along with convolution is used to obtain the analytical results for the velocity, microrotations, temperature and concentration profiles. The obtained results are plotted to see the effects of indispensable flow parameters and discussed in detail. Skin friction, wall couple stress, Nusselt number and Sherwood number are also computed. Validation of the analysis has been performed by comparing the present results with those of Chaudhary and Jain [6].

Mathematical formulation

Consider the unsteady boundary layer flow of an incompressible micropolar fluid in the region $y > 0$ driven by a plane surface located at $y = 0$ with a fixed end at $x = 0$. The fluid is electrically conducting and passing through a porous medium. It is assumed that at the initial moment $t = 0$, both the plate and the fluid are at rest at the constant temperature T_∞ and concentration C_∞. At time $t = 0^+$, the plate begins to oscillate in its plane ($y = 0$) according to

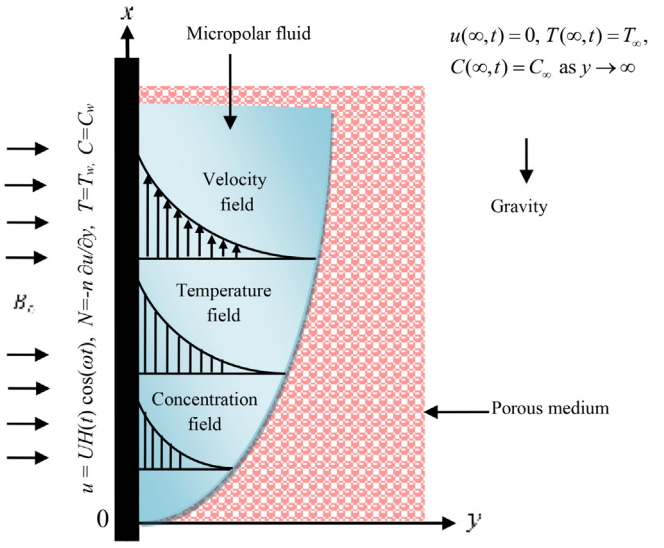

Fig. 1. Flow configuration of the problem.

$$\boldsymbol{V} = UH(t)\cos(\omega t)\mathbf{i}; t > 0, \tag{1}$$

where $H(t)$ is the unit step function, U is the amplitude of the motion, $\mathbf{i}$ is the unit vector in the vertical flow direction and ω is the frequency of oscillation of the plate. The fluid is assumed to be electrically conducting with a uniform magnetic field $\boldsymbol{B}$ of strength B_0, applied in a direction perpendicular to the plate. At the same time, the plate temperature and concentration level are raised to T_w and C_w which are thereafter maintained constants (see Fig. 1).

Assume that the velocity, temperature and concentration are functions of y and t only. Taking the usual Boussinesq's approximation and the viscous dissipation term in the energy equation is neglected, magnetic Reynolds number is small, electric field is zero and the unsteady incompressible flow is governed by the following set of partial differential equations:

$$\rho\frac{\partial u}{\partial t} = (\mu + \alpha)\frac{\partial^2 u}{\partial y^2} - \sigma B_0^2 u - \frac{\mu\zeta}{k_1}u + \rho g\beta_T(T - T_\infty) + \rho g\beta_C(C - C_\infty) + \alpha\frac{\partial N}{\partial y}, \tag{2}$$

$$\rho\, j\frac{\partial N}{\partial t} = \gamma\frac{\partial^2 N}{\partial y^2}, \tag{3}$$

$$\rho C_p\frac{\partial T}{\partial t} = k\frac{\partial^2 T}{\partial y^2}, \tag{4}$$

$$\frac{\partial C}{\partial t} = D\frac{\partial^2 C}{\partial y^2}. \tag{5}$$

The corresponding initial and boundary conditions are given as

$$\begin{aligned} &u(y,0) = 0,\ N(y,0) = 0, T(y,0) = T_\infty, C(y,0) = C_\infty \text{ for all } y \geqslant 0,\\ &u(0,t) = H(t)U\cos(\omega t), N(0,t) = -n\tfrac{\partial u}{\partial y}(0,t), T_\infty(0,t) = T_w \text{ and } C(0,t)\\ &\qquad = C_w, t > 0,\\ &u(\infty,t) \to 0,\ N(\infty,t) \to 0, T(\infty,t) \to T_\infty \text{ and } C(\infty,t) \to C_\infty \text{ as } y \to \infty. \end{aligned} \tag{6}$$

Here u is velocity, μ is dynamic viscosity, ρ is density, g is gravitational acceleration, α is vortex viscosity, t is time, T is the temperature, C is the species concentration, D is the mass diffusivity, σ the electrical conductivity of the fluid, k_1 permeability of the fluid, ζ is the porosity of fluid, β_T is volumetric coefficient of thermal expansion, β_C is volumetric coefficient of expansion with concentration, N is the microrotation

whose direction of rotation is in the xy-plane, j is microinertia per unit mass, γ is spin gradient viscosity, C_p is heat capacity at constant pressure, k is thermal conductivity, ωt is phase angle q_r is the radiative heat flux. Three different values of $0 \leqslant n \leqslant 1$, when $n = 0$, which indicates $N = 0$ at the wall represents concentrated particle flows in which the microelements close to the wall surface are unable to rotate, this situation is also known as strong concentration of microelements. When $n = 1/2$, it indicates the vanishing of anti-symmetric part of the stress tensor and denotes weak concentration of microelements. The last case when $n = 1$ is used for the modelling of turbulent boundary layer flows [27]. The spin gradient viscosity γ, measures the relationship between the coefficients of viscosity and micro-inertia, is defined as

$$\gamma = \left(\mu + \frac{\alpha}{2}\right), j = \mu j\left(1 + \frac{\beta}{2}\right) \text{ and } \beta = \frac{\alpha}{\mu}.$$

To reduce the above Eqs. (2)–(5) into their non-dimensional forms, following non-dimensional quantities are established,

$$y^{*}= \frac{U}{\nu}y,\ t^{*} = \frac{U^2}{\nu}t,\ u^{*} = \frac{u}{U},\ N^{*} = \frac{\nu}{U^2}N,\ \theta = \frac{T - T_\infty}{T_w - T_\infty},$$
$$\phi= \frac{C - C_\infty}{C_w - C_\infty},\ \omega^{*} = \frac{\nu}{U^2}\omega,\ j^{*} = \frac{U^2}{\nu^2}j. \tag{7}$$

Implementing Eq. (7) into Eq. (2)–(5), we obtain the following non-dimensional partial differential equations (* symbol is omitted for simplicity)

$$\frac{\partial u}{\partial t} = (1 + \beta)\frac{\partial^2 u}{\partial y^2} - \left(M + \frac{1}{K}\right)u + \beta\frac{\partial N}{\partial y} + Gr\theta + Gm\phi, \tag{8}$$

$$\frac{\partial N}{\partial t} = \frac{1}{\eta}\frac{\partial^2 N}{\partial y^2}, \tag{9}$$

$$\frac{\partial \theta}{\partial t} = \frac{1}{\mathrm{Pr}}\frac{\partial^2 \theta}{\partial y^2}, \tag{10}$$

$$\frac{\partial \phi}{\partial t} = \frac{1}{Sc}\frac{\partial^2 \phi}{\partial y^2}. \tag{11}$$

The corresponding initial and boundary conditions take the following non-dimensional forms:

$$u(y,0) = 0,\ N(y,0) = 0, \theta(y,0) = 0,\ \phi(y,0) = 0 \text{ for all } y \geqslant 0,$$
$$u(0,t) = H(t)\cos(\omega t),\ N(0,t) = -n\frac{\partial u}{\partial y}(0,t), \theta(0,t) = 1,\ \phi(0,t) = 1, t > 0,$$
$$u(\infty,t) \to 0,\ N(\infty,t) \to 0, \theta(\infty,t) \to 0,\ \phi(\infty,t) \to 0 \ as\ y \to \infty. \tag{12}$$

where

$$M = \frac{\sigma\nu B_0^2}{\rho U^2},\ \frac{1}{K} = \frac{\nu^2\zeta}{k_1 U^2}, Gr = \frac{g\beta_T(T_w - T_\infty)\nu}{U^3}, Gm = \frac{g\beta_C(C_w - C_\infty)\nu}{U^3},$$
$$\eta = \frac{\mu j}{\gamma}, \mathrm{Pr} = \frac{\mu C_p}{k}, Sc = \frac{\nu}{D},$$

are the magnetic parameter, permeability parameter, Grashof number, modified Grashof number, microrotation parameter, dimensionless spin gradient, Prandtl number and Schmidt number, respectively.

Exact solutions

Applying the Laplace transforms to Eqs. (8)–(11), and using conditions (12), the following solutions in the transformed (y,q) plane are obtained:

$$q\overline{u}(y,q) = (1 + \beta)\frac{d^2\overline{u}(y,q)}{dy^2} + \beta\frac{d\overline{N}(y,q)}{dy} - \left(M + \frac{1}{K}\right)\overline{u}(y,q) + Gr\overline{\theta}(y,q) + Gm\overline{\phi}(y,q), \tag{13}$$

$$\overline{N}(y,q) = \frac{1}{\eta}\frac{d^2\overline{N}(y,q)}{dy^2}, \tag{14}$$

$$\overline{\theta}(y,q) = \frac{1}{\mathrm{Pr}}\frac{d^2\overline{\theta}(y,q)}{dy^2}, \tag{15}$$

$$\overline{\phi}(y,q) = \frac{1}{Sc}\frac{d^2\overline{\phi}(y,q)}{dy^2}, \tag{16}$$

with transformed boundary conditions are

$$\overline{u}(\infty,q) = 0,\ \overline{N}(\infty,q) = 0, \overline{\phi}(\infty,q) = 0,$$
$$\overline{u}(y,q) = \frac{q}{q^2 + w^2}, \overline{N}(0,q) = -n\frac{d\overline{u}(0,q)}{dy}, \overline{\theta}(0,q) = \frac{1}{q}, \overline{\phi}(0,q) = \frac{1}{q}. \tag{17}$$

Solutions of Eqs. (15) and (16) under the corresponding boundary conditions in Eq. (17) are:

$$\overline{\theta}(y,q) = \frac{1}{q}e^{-y\sqrt{\mathrm{Prq}}}, \tag{18}$$

$$\overline{\phi}(y,q) = \frac{1}{q}e^{-y\sqrt{Scq}}. \tag{19}$$

Inverse Laplace transform of Eqs. (18) and (19) are given as:

$$\theta(y,t) = \mathrm{erfc}\left(\frac{y\sqrt{\mathrm{Pr}}}{2\sqrt{t}}\right), \tag{20}$$

$$\phi(y,t) = \mathrm{erfc}\left(\frac{y\sqrt{Sc}}{2\sqrt{t}}\right). \tag{21}$$

Solution of Eqs. (13) and (14) with corresponding boundary conditions from Eq. (17) and in view of Eqs. (20) and (21), is given by:

$$\overline{u}(y,q) = \overline{u}_1(y,q) + \overline{u}_2(y,q) + \overline{u}_3(y,q) - \overline{u}_4(y,q) + \overline{u}_5(y,q), \tag{22}$$

$$\overline{N}(y,q) = \overline{N}_1(y,q) + \overline{N}_2(y,q), \tag{23}$$

where

$$\begin{aligned}\overline{u}_1(y,q) = {} & \Re_0\overline{\varphi}(y\sqrt{\beta_0},q,-i\omega,k_0) + \Re_1\overline{\varphi}(y\sqrt{\beta_0},q,i\omega,k_0) - \Re_2\overline{\varphi}(y\sqrt{\beta_0},q,0,k_0) \\ & + \Re_3\overline{\varphi}(y\sqrt{\beta_0},q,a_{11},k_0) + \Re_4\overline{\varphi}(y\sqrt{\beta_0},q,a_{12},k_0) \\ & - \Re_5\overline{\varphi}(y\sqrt{\beta_0},q,-\delta_1,k_0) - \Re_6\overline{\varphi}(y\sqrt{\beta_0},q,-\delta_2,k_0) \\ & - \Re_7\overline{\varphi}(y\sqrt{\beta_0},q,\delta_3,k_0),\end{aligned}$$

$$\begin{aligned}\overline{u}_2(y,q) = {} & \Re_7\overline{\varphi}(y\sqrt{\eta},q,\delta_3,0) + \Re_8\overline{\varphi}(y\sqrt{\eta},q,a_{11},0) + \Re_9\overline{\varphi}(y\sqrt{\eta},q,a_{12},0) \\ & + \Re_5\overline{\varphi}(y\sqrt{\eta},q,-\delta_1,0) + \Re_6\overline{\varphi}(y\sqrt{\eta},q,-\delta_2,0) + \Re_{10}\overline{\varphi}(y\sqrt{\eta},q,i\omega,0) \\ & + \Re_{11}\overline{\varphi}(y\sqrt{\eta},q,-i\omega,0),\end{aligned}$$

$$\begin{aligned}\overline{u}_3(y,q) = {} & \lambda_0\overline{\varphi}(y\sqrt{\mathrm{Pr}},t,0,0) - \lambda_0\overline{\varphi}(y\sqrt{\mathrm{Pr}},t,a_{11},0) + \lambda_1\overline{\varphi}(y\sqrt{Sc},t,0,0) \\ & - \lambda_1\overline{\varphi}(y\sqrt{Sc},t,a_{12},0),\end{aligned}$$

$$\overline{u}_4(y,q) = \sqrt{q}\begin{bmatrix}\Re_{12}\overline{\psi}(y\sqrt{\beta_0},q,0,k_0) + \Re_{13}\overline{\psi}(y\sqrt{\beta_0},q,\delta_3,k_0) \\ \quad + \Re_{14}\overline{\psi}(y\sqrt{\beta_0},q,a_{11},k_0) \\ + \Re_{15}\overline{\psi}(y\sqrt{\beta_0},q,a_{12},k_0) + \Re_{16}\overline{\psi}(y\sqrt{\beta_0},q,-\delta_1,k_0) \\ \quad - \Re_{17}\overline{\psi}(y\sqrt{\beta_0},q,-\delta_2,k_0) \\ + \Re_{18}\overline{\psi}(y\sqrt{\beta_0},q,i\omega,k_0) - \Re_{19}\overline{\psi}(y\sqrt{\beta_0},q,-i\omega,k_0)\end{bmatrix},$$

$$\overline{u}_5(y,q) = \sqrt{q + k_0}\begin{bmatrix}\Re_{12}\overline{\psi}(y\sqrt{\eta},q,0,0) + \Re_{13}\overline{\psi}(y\sqrt{\eta},q,\delta_3,0) \\ \quad + \Re_{14}\overline{\psi}(y\sqrt{\eta},q,a_{11},0) \\ + \Re_{15}\overline{\psi}(y\sqrt{\eta},q,a_{12},0) + \Re_{16}\overline{\psi}(y\sqrt{\eta},q,-\delta_1,0) \\ \quad - \Re_{17}\overline{\psi}(y\sqrt{\eta},q,-\delta_2,0) \\ + \Re_{18}\overline{\psi}(y\sqrt{\eta},q,i\omega,0) - \Re_{19}\overline{\psi}(y\sqrt{\eta},q,-i\omega,0)\end{bmatrix},$$

$$\overline{N}_1(y,q) = n\sqrt{\beta_0}\sqrt{q+k_0}\begin{bmatrix} L_1\overline{\varphi}(y\sqrt{\eta},q,0,0) + L_2\overline{\varphi}(y\sqrt{\eta},q,a_{11},0) \\ + L_3\overline{\varphi}(y\sqrt{\eta},q,a_{12},0) + L_4\overline{\varphi}(y\sqrt{\eta},q,-\delta_1,0) \\ + L_5\overline{\varphi}(y\sqrt{\eta},q,-\delta_2,0) + L_6\overline{\varphi}(y\sqrt{\eta},q,i\omega,0) \\ + L_7\overline{\varphi}(y\sqrt{\eta},q,-i\omega,0) \end{bmatrix},$$

$$\overline{N}_2(y,q) = n\begin{bmatrix} L_8\overline{\psi}(y\sqrt{\eta},q,0,0) + L_9\overline{\psi}(y\sqrt{\eta},q,a_{11},0) \\ + L_{10}\overline{\psi}(y\sqrt{\eta},q,a_{12},0) + L_{11}\overline{\psi}(y\sqrt{\eta},q,-\delta_1,0) \\ + L_{12}\overline{\psi}(y\sqrt{\eta},q,-\delta_2,0) + L_{13}\overline{\psi}(y\sqrt{\eta},q,i\omega,0) \\ + L_{14}\overline{\psi}(y\sqrt{\eta},q,\delta_3,0) \end{bmatrix},$$

$$\overline{\varphi}(\xi,q,\lambda,b) = \frac{1}{q-\lambda}\exp(-\xi\sqrt{q+b}),$$

$$\overline{\psi}(\xi,q,\lambda,b) = \frac{\sqrt{q+b}}{q-\lambda}\exp(-\xi\sqrt{q+b}).$$

For $\Re_i$, i = 1,2...19 and L_j, j = 1,2...14, see Appendix.

Following Hetnarski [36], the Laplace inverse transforms of Eqs. (22) and (23) are given by:

$$u(y,t) = u_1(y,t) + u_2(y,t) + u_3(y,t) - u_4(y,t) + u_5(y,t), \tag{24}$$

$$N(y,t) = N_1(y,t) + N_2(y,t), \tag{25}$$

where

$$u_1(y,t) = \Re_0\varphi(y\sqrt{\beta_0},t,-i\omega,k_0) + \Re_1\varphi(y\sqrt{\beta_0},t,i\omega,k_0) - \Re_2\varphi(y\sqrt{\beta_0},t,0,k_0) + \Re_3\varphi(y\sqrt{\beta_0},t,a_{11},k_0) + \Re_4\varphi(y\sqrt{\beta_0},t,a_{12},k_0) - \Re_5\varphi(y\sqrt{\beta_0},t,-\delta_1,k_0) + \Re_6\varphi(y\sqrt{\beta_0},t,-\delta_2,k_0) - \Re_7\varphi(y\sqrt{\beta_0},t,\delta_3,k_0),$$

$$u_2(y,t) = \Re_7\varphi(y\sqrt{\eta},t,\delta_3,0) + \Re_8\varphi(y\sqrt{\eta},t,a_{11},0) + \Re_9\varphi(y\sqrt{\eta},t,a_{12},0) + \Re_5\varphi(y\sqrt{\eta},t,-\delta_1,0) + \Re_6\varphi(y\sqrt{\eta},t,-\delta_2,0) + \Re_{10}\varphi(y\sqrt{\eta},t,i\omega,0) + \Re_{11}\varphi(y\sqrt{\eta},t,-i\omega,0),$$

$$u_3(y,t) = \lambda_0\varphi(y\sqrt{\mathrm{Pr}},t,0,0) - \lambda_0\varphi(y\sqrt{\mathrm{Pr}},t,a_{11},0) + \lambda_1\varphi(y\sqrt{Sc},t,0,0) - \lambda_1\varphi(y\sqrt{Sc},t,a_{12},0),$$

$$u_4(y,t) = -\left(\frac{1}{2t\sqrt{\pi t}}\right) * \begin{bmatrix} \Re_{12}\psi(y\sqrt{\beta_0},t,0,k_0) + \Re_{13}\psi(y\sqrt{\beta_0},t,\delta_3,k_0) \\ + \Re_{14}\psi(y\sqrt{\beta_0},t,a_{11},k_0) + \Re_{15}\psi(y\sqrt{\beta_0},t,a_{12},k_0) \\ + \Re_{16}\psi(y\sqrt{\beta_0},t,-\delta_1,k_0) - \Re_{17}\psi(y\sqrt{\beta_0},t,-\delta_2,k_0) \\ + \Re_{18}\psi(y\sqrt{\beta_0},t,i\omega,k_0) - \Re_{19}\psi(y\sqrt{\beta_0},t,-i\omega,k_0) \end{bmatrix},$$

$$u_5(y,t) = -\left(\frac{1}{2t\sqrt{\pi t}}e^{-k_0 t}\right) * \begin{bmatrix} \Re_{12}\psi(y\sqrt{\beta_0},t,0,0) + \Re_{13}\psi(y\sqrt{\beta_0},t,\delta_3,0) \\ + \Re_{14}\psi(y\sqrt{\beta_0},t,a_{11},0) + \Re_{15}\psi(y\sqrt{\beta_0},t,a_{12},0) \\ + \Re_{16}\psi(y\sqrt{\beta_0},t,-\delta_1,0) - \Re_{17}\psi(y\sqrt{\beta_0},t,-\delta_2,0) \\ + \Re_{18}\psi(y\sqrt{\beta_0},t,i\omega,0) - \Re_{19}\psi(y\sqrt{\beta_0},t,-i\omega,0) \end{bmatrix},$$

$$N_1(y,t) = -n\sqrt{\beta_0}\left(\frac{1}{2t\sqrt{\pi t}}e^{-k_0 t}\right) * \begin{bmatrix} L_1\varphi(y\sqrt{\eta},t,0,0) + L_2\varphi(y\sqrt{\eta},t,a_{11},0) \\ + L_3\varphi(y\sqrt{\eta},t,a_{12},0) + L_4\varphi(y\sqrt{\eta},t,-\delta_1,0) \\ + L_5\varphi(y\sqrt{\eta},t,-\delta_2,0) + L_6\varphi(y\sqrt{\eta},t,i\omega,0) \\ + L_7\varphi(y\sqrt{\eta},t,-i\omega,0) \end{bmatrix},$$

$$N_2(y,t) = n\begin{bmatrix} L_8\psi(y\sqrt{\eta},t,0,0) + L_9\psi(y\sqrt{\eta},t,a_{11},0) + L_{10}\psi(y\sqrt{\eta},t,a_{12},0) \\ + L_{11}\psi(y\sqrt{\eta},t,-\delta_1,0) + L_{12}\psi(y\sqrt{\eta},t,-\delta_2,0) \\ \quad + L_{13}\psi(y\sqrt{\eta},t,i\omega,0) \\ + L_{14}\psi(y\sqrt{\eta},t,\delta_3,0) \end{bmatrix},$$

$$\varphi(\xi,t,\lambda,b) = \frac{\exp(\lambda t)}{2}\begin{bmatrix} \exp(-\xi\sqrt{\lambda+b})\mathrm{erfc}(\frac{\xi}{2\sqrt{t}} - \sqrt{(\lambda+b)t}) \\ + \exp(\xi\sqrt{\lambda+b})\mathrm{erfc}(\frac{\xi}{2\sqrt{t}} + \sqrt{(\lambda+b)t}) \end{bmatrix},$$

$$\psi(\xi,t,\lambda,b) = (\lambda+b)\frac{\exp(\lambda t)}{2\sqrt{\lambda+b}}\begin{bmatrix} \exp(-\xi\sqrt{\lambda+b})\mathrm{erfc}(\frac{\xi}{2\sqrt{t}} - \sqrt{(\lambda+b)t}) \\ - \exp(\xi\sqrt{\lambda+b})\mathrm{erfc}(\frac{\xi}{2\sqrt{t}} + \sqrt{(\lambda+b)t}) \end{bmatrix} + \frac{1}{\sqrt{\pi t}}\exp\left(-\frac{\xi^2}{4t} - bt\right),$$

here the $f*g$ shows the convolution product of f and g.

Skin friction and wall couple stress

The skin friction co-efficient at the wall is:

$$\tau = -\left(1 + \frac{1}{\alpha}\right)\frac{\partial u}{\partial y}\bigg|_{y=0} + \alpha N|_{y=0},$$

which in dimensionless form reduces to:

$$C_f = \frac{2\tau_w^*}{\rho U^2} = 2[1 + (1-n) + \beta]u'(0). \tag{26}$$

Similarly, the dimensionless couple wall stress co-efficient at the plate is expressed as:

$$C_m = \gamma\frac{\partial N}{\partial y}\bigg|_{y=0},$$

and in dimensionless form is:

$$C_m^* = \frac{C_m}{\mu j U} = (1+\beta)N'(0). \tag{27}$$

The Nusselt number and Sherwood number can be calculated as:

$$Nu = x\frac{(\partial T/\partial y^*)y^*}{T_\infty - T_w} = 0,$$

$$Nu\ \mathrm{Re}_x^{-1} = -\theta'(0), \tag{28}$$

$$Sh = x\frac{(\partial C/\partial y^*)y^*}{C_\infty - C_w} = 0,$$

$$Sh\ \mathrm{Re}_x^{-1} = -\phi'(0), \tag{29}$$

where $\mathrm{Re}_x = \frac{wx}{U}$ is the local Reynolds number.

Limiting cases

The following solutions from the literature appear as the limiting cases of obtained general solutions.

Solution in the absence of free convection

In this case we assume that, the flow is induced only due to bounding plate. The corresponding buoyancy forces are zero equivalently, this shows the absence of free convection, which numerically corresponds to $Gr = 0$ and $Gm = 0$ due to the differences in the temperature gradient. Clearly, in this case the thermal parts of velocities are zero. Hence the flow is only governed by the corresponding mechanical parts given by

$$u(y,t) = u_1'(y,t) + u_2'(y,t), \tag{30}$$

where

$$u_1'(y,t) = \Re_0\varphi(y\sqrt{\beta_0},t,-i\omega,k_0) + \Re_1\varphi(y\sqrt{\beta_0},t,i\omega,k_0),$$

$$u_2'(y,t) = \Re_{10}\varphi(y\sqrt{\eta},t,i\omega,0) + \Re_{11}\varphi(y\sqrt{\eta},t,-i\omega,0).$$

Solution in the absence of mechanical effects

In this case, consider the flow situation when the infinite plate is static position at every time. More exactly, the wall velocity of the fluid

is zero for each real value of t and thus the mechanical component of velocity identically vanishes. Consequently, the velocity of the fluid $u(y,t)$ reduces to its thermal components velocity as

$$u(y,t) = u_1''(y,t) + u_2''(y,t) + u_3(y,t) - u_4''(y,t) + u_5''(y,t), \tag{31}$$

where

$$u_1''(y,t) = -\Re_2\varphi(y\sqrt{\beta_0},t,0,k_0) + \Re_3\varphi(y\sqrt{\beta_0},t,a_{11},k_0) + \Re_4\varphi(y\sqrt{\beta_0},t,a_{12},k_0) - \Re_5\varphi(y\sqrt{\beta_0},t,-\delta_1,k_0) - \Re_6\varphi(y\sqrt{\beta_0},t,-\delta_2,k_0) - \Re_7\varphi(y\sqrt{\beta_0},t,\delta_3,k_0),$$

$$u_2''(y,t) = \Re_7\varphi(y\sqrt{\eta},t,\delta_3,0) + \Re_8\varphi(y\sqrt{\eta},t,a_{11},0) + \Re_9\varphi(y\sqrt{\eta},t,a_{12},0) + \Re_5\varphi(y\sqrt{\eta},t,-\delta_1,0) + \Re_6\varphi(y\sqrt{\eta},t,-\delta_2,0),$$

$$u_4''(y,t) = -\left(\frac{1}{2t\sqrt{\pi t}}\right) * \begin{bmatrix} \Re_{12}\psi(y\sqrt{\beta_0},t,0,k_0) + \Re_{15}\psi(y\sqrt{\beta_0},t,a_{12},k_0) \\ + \Re_{16}\psi(y\sqrt{\beta_0},t,-\delta_1,k_0) - \Re_{17}\psi(y\sqrt{\beta_0},t,-\delta_2,k_0) \end{bmatrix},$$

$$u_5''(y,t) = -\left(\frac{1}{2t\sqrt{\pi t}}e^{-k_0 t}\right) * \begin{bmatrix} \Re_{12}\psi(y\sqrt{\beta_0},t,0,0) + \Re_{15}\psi(y\sqrt{\beta_0},t,a_{12},0) \\ + \Re_{16}\psi(y\sqrt{\beta_0},t,-\delta_1,0) - \Re_{17}\psi(y\sqrt{\beta_0},t,-\delta_2,0) \end{bmatrix}.$$

Solution in the absence of MHD and porosity effects

In this problem, temperature and concentration distributions are not effected by MHD and porosity effects. However, MHD and porosity have strong influence on velocity as it can be seen from Eq. (24). Thus, in the absence of MHD and porosity effects, Eq. (24) reduces to

$$u(y,t) = u_1'''(y,t) + u_2'''(y,t) - u_4'''(y,t) + u_5'''(y,t), \tag{32}$$

where

$$u_1'''(y,t) = \Re_0\varphi(y\sqrt{\beta_0},t,-i\omega,0) + \Re_1\varphi(y\sqrt{\beta_0},t,i\omega,0) + \Re_5\varphi(y\sqrt{\beta_0},t,-\delta_1,0) + \Re_6\varphi(y\sqrt{\beta_0},t,-\delta_2,0),$$

$$u_2'''(y,t) = \Re_5\varphi(y\sqrt{\eta},t,-\delta_1,0) + \Re_6\varphi(y\sqrt{\eta},t,-\delta_2,0) + \Re_{10}\varphi(y\sqrt{\eta},t,i\omega,0) + \Re_{11}\varphi(y\sqrt{\eta},t,-i\omega,0),$$

$$u_4'''(y,t) = -\left(\frac{1}{2t\sqrt{\pi t}}\right) * \begin{bmatrix} \Re_{16}\psi(y\sqrt{\beta_0},t,-\delta_1,0) - \Re_{17}\psi(y\sqrt{\beta_0},t,-\delta_2,0) \\ + \Re_{18}\psi(y\sqrt{\beta_0},t,i\omega,0) - \Re_{19}\psi(y\sqrt{\beta_0},t,-i\omega,0) \end{bmatrix},$$

$$u_5'''(y,t) = -\left(\frac{1}{2t\sqrt{\pi t}}\right) * \begin{bmatrix} \Re_{16}\psi(y\sqrt{\beta_0},t,-\delta_1,0) - \Re_{17}\psi(y\sqrt{\beta_0},t,-\delta_2,0) \\ + \Re_{18}\psi(y\sqrt{\beta_0},t,i\omega,0) - \Re_{19}\psi(y\sqrt{\beta_0},t,-i\omega,0) \end{bmatrix}.$$

Solutions for Stokes first problem

In this limiting case, the flow in the fluid is induced due to impulsive motion of the plate. Thus taking $\omega t = \beta = \eta = 0$ and $n = 0.00001$ (equivalently $n \to 0$) into Eq. (24), which correspond the impulsive motion of the plate as:

$$u(y,t) = \underset{\sim}{u}_1(y,t) + u_3(y,t), \tag{33}$$

where

$$\underset{\sim}{u}_1(y,t) = \Re_0\varphi(y\sqrt{\beta_0},t,-i\omega,k_0) + \Re_1\varphi(y\sqrt{\beta_0},t,i\omega,k_0) - \Re_2\varphi(y\sqrt{\beta_0},t,0,k_0) + \Re_3\varphi(y\sqrt{\beta_0},t,a_{11},k_0) + \Re_4\varphi(y\sqrt{\beta_0},t,a_{12},k_0).$$

It is important to note that Eq. (33) is found identical to those obtained by Chaudhary and Jain [6], Eq. (19). Hence this verifies the correctness of the present work. This comparison is graphically shown in Fig. 26.

Results and discussion

To assess the physical properties of the present problem, the effects of various parameters like microrotation parameter β, spin gradient viscosity parameter η, microelement n, Prandtl number Pr, Grashof number Gr, modified Grashof number Gm, magnetic parameter M, permeability of porous medium K, Schmidt number Sc, phase angle ωt and time t are analyzed. Numerical results of skin friction, wall couple stress, Nusselt number and Sherwood number are also presented in tables (see Tables 1–4).

Table 1
Variations of skin friction.

β	η	n	Pr	Gr	Gm	M	K	Sc	ωt	t	τ
0.5	0.6	0.6	10	5.0	5.0	0.5	0.5	0.2	$\pi/4$	0.6	3.4781
2.0	0.6	0.6	10	5.0	5.0	0.5	0.5	0.2	$\pi/4$	0.6	3.8136
0.5	**0.9**	0.6	10	5.0	5.0	0.5	0.5	0.2	$\pi/4$	0.6	3.0452
0.5	0.6	**0.9**	10	5.0	5.0	0.5	0.5	0.2	$\pi/4$	0.6	2.9321
0.5	0.6	0.6	**15**	5.0	5.0	0.5	0.5	0.2	$\pi/4$	0.6	3.6112
0.5	0.6	0.6	10	**7.0**	5.0	0.5	0.5	0.2	$\pi/4$	0.6	3.1576
0.5	0.6	0.6	10	5.0	**7.0**	0.5	0.5	0.2	$\pi/4$	0.6	3.1762
0.5	0.6	0.6	10	5.0	5.0	**1.5**	0.5	0.2	$\pi/4$	0.6	3.6238
0.5	0.6	0.6	10	5.0	5.0	0.5	**1.5**	0.2	$\pi/4$	0.6	2.7756
0.5	0.6	0.6	10	5.0	5.0	0.5	0.5	**0.5**	$\pi/4$	0.6	3.5342
0.5	0.6	0.6	10	5.0	5.0	0.5	0.5	0.2	$\boldsymbol{\pi/2}$	0.6	3.5681
0.5	0.6	0.6	10	5.0	5.0	0.5	0.5	0.2	$\pi/4$	**0.9**	2.9872

Bold values indicate the variation in the corresponding parameter in each column.

The effect of β on velocity and the microrotation is plotted in Figs. 2 and 3. These graphs show that velocity decreases whereas microrotation increases with increasing β. On the other hand, the microrotation takes the negative values of the gradient of velocity at the plate surface and approaching to zero as one move away from the plate surface as shown in Fig. 3. This fact totally aggress with imposed conditions on microrotation (see Eq. (17)). The influence of spin gradient viscosity parameter η on the velocity and microrotation is plotted in Figs. 4 and 5. It is found that velocity increases with increasing η, while reverse effect is observed for microrotation. Figs. 6 and 7 reveal the effect of parameter n, which relates to the microgyration vector and the shear stress on the linear velocity and the microrotation profiles. It is observed that velocity increases with increasing values of n, whereas the magnitude of the microrotation increases with an increase of n close to the plate but decreases with increasing distance from the plate.

Figs. 8–10 elucidate the effect of Pr on velocity, microrotations and temperature profiles. These graphs explain that the influence of increasing values of Pr result in decreasing of the velocity and temperature. Physically, this is due to the smaller values of Pr increase the thermal conductivity of the fluid and consequently heat is able to diffuse away more rapidly for higher values of Pr from the heated surface. On the other hand, Fig. 9 shows that the magnitude of microrotation increases as Pr increases. Figs. 11 and 12 displays variations in velocity and microrotation profiles for various values of Gr. It is noted that an increase in Gr leads to an increase in velocity due to enhancement in the buoyancy force. Besides that magnitude of microrotation decreases for large values of Gr. Positive values of Gr correspond to cooling of the surface by natural convection whereas $Gr = 0$ shows the absence of heat transfer due to free convection. On the other hand, the sketches of velocity and microrotation for different values of Gm, are shown in Figs. 13 and 14. It is observed that, velocity distribution achieves a

Table 2
Variations of Nusselt number.

Pr	t	Nu
10	0.3	0.564
15	0.3	0.867
10	**0.6**	0.398

Bold values indicate the variation in the corresponding parameter in each column.

Table 3
Variations of wall couple stress.

β	η	n	Pr	Gr	Gm	M	K	Sc	ωt	t	C_m
0.5	0.6	0.6	10	5.0	5.0	0.5	0.5	0.2	$\pi/4$	0.6	3.5681
2.0	0.6	0.6	10	5.0	5.0	0.5	0.5	0.2	$\pi/4$	0.6	2.2043
0.5	**0.9**	0.6	10	5.0	5.0	0.5	0.5	0.2	$\pi/4$	0.6	2.1090
0.5	0.6	**0.9**	10	5.0	5.0	0.5	0.5	0.2	$\pi/4$	0.6	2.5378
0.5	0.6	0.6	**15**	5.0	5.0	0.5	0.5	0.2	$\pi/4$	0.6	3.0723
0.5	0.6	0.6	10	**7.0**	5.0	0.5	0.5	0.2	$\pi/4$	0.6	1.9087
0.5	0.6	0.6	10	5.0	**7.0**	0.5	0.5	0.2	$\pi/4$	0.6	2.6540
0.5	0.6	0.6	10	5.0	5.0	**1.5**	0.5	0.2	$\pi/4$	0.6	3.6321
0.5	0.6	0.6	10	5.0	5.0	0.5	**1.5**	0.2	$\pi/4$	0.6	2.6732
0.5	0.6	0.6	10	5.0	5.0	0.5	0.5	**0.5**	$\pi/4$	0.6	3.0684
0.5	0.6	0.6	10	5.0	5.0	0.5	0.5	0.2	$\pi/2$	0.6	2.7612
0.5	0.6	0.6	10	5.0	5.0	0.5	0.5	0.2	$\pi/4$	**0.9**	2.349

Bold values indicate the variation in the corresponding parameter in each column.

Table 4
Variations of Sherwood number.

Sc	t	Sh
0.2	0.6	0.2312
0.6	0.6	0.2754
0.2	**0.8**	0.2167

Bold values indicate the variation in the corresponding parameter in each column.

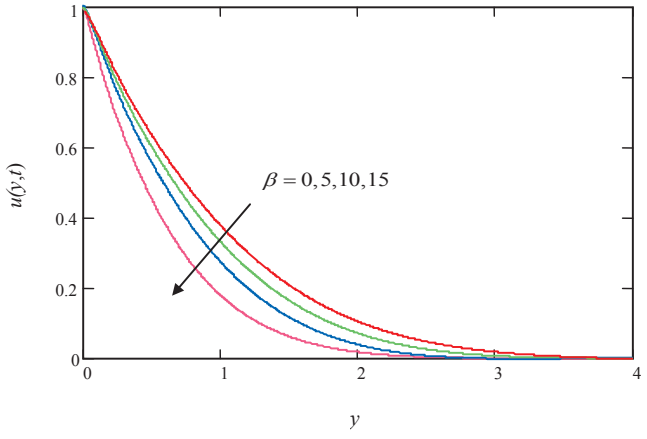

Fig. 2. Profiles of velocity for different values of β when $\eta = 1.5, n = 0.6, \mathrm{Pr} = 15, Gr = Gm = 5, M = K = 0.5, Sc = 0.2, \omega t = 0$ and $t = 0.6$.

maximum value in the neighborhood of the plate because of an increase in the buoyancy force due to concentration gradient and then decreases accurately to move towards a free stream value. The curve corresponding to $Gm = 0$ shows the absence of free convection due to mass transfer.

For different values of M, the velocity and microrotation profiles are plotted in Figs. 15 and 16. It is found that the increasing of the magnetic field is due to decreasing values of the velocity profiles throughout the boundary layer. The effect of the magnetic field is more prominent at the point of the peak value, i.e., the peak value drastically decreases with an increase in the value of the magnetic field, because the presence of the magnetic field in an electrically conducting fluid introduces a force called the Lorentz force, which acts against the flow if the magnetic field is applied in the normal direction, as in the present problem. This type of resisting force slows down the fluid velocity as shown in

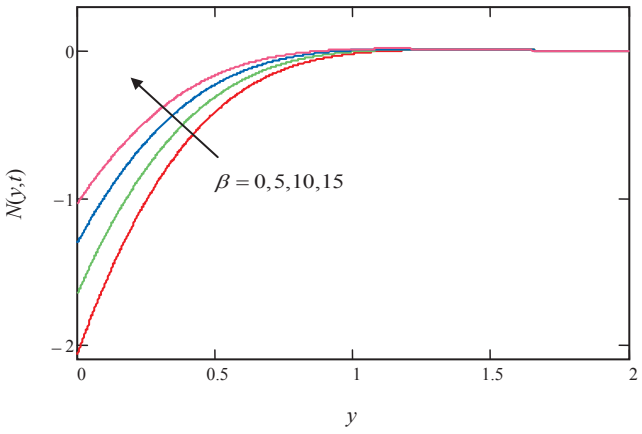

Fig. 3. Profiles of microrotations for different values of β when $\eta = 1.5, n = 0.6, \mathrm{Pr} = 15, Gr = Gm = 5, M = K = 0.5, Sc = 0.2, \omega t = 0$ and $t = 0.6$.

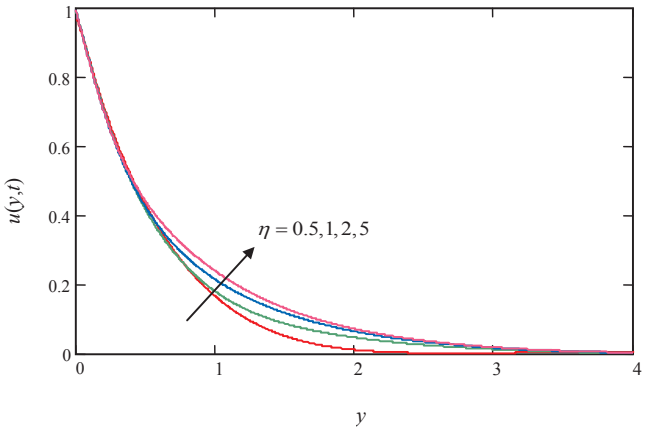

Fig. 4. Profiles of velocity for different values of η when $\beta = 0.5, n = 0.6, \mathrm{Pr} = 15, Gr = Gm = 5, M = K = 0.5, Sc = 0.2, \omega t = 0$ and $t = 0.6$.

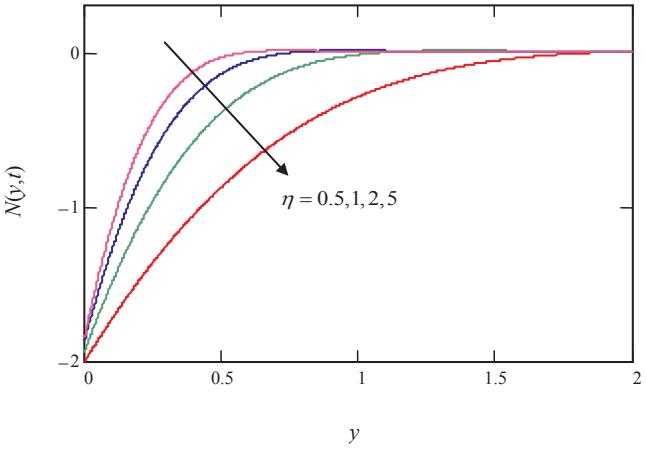

Fig. 5. Profiles of microrotations for different values of η when $\beta = 0.5, n = 0.6, \mathrm{Pr} = 15, Gr = Gm = 5, M = K = 0.5, Sc = 0.2, \omega t = 0$ and $t = 0.6$.

this figure. In contrast, the results show that the magnitude of the microrotation decreases as M increases. For various values of the K, the profiles of the velocity and the microrotation across the boundary layer

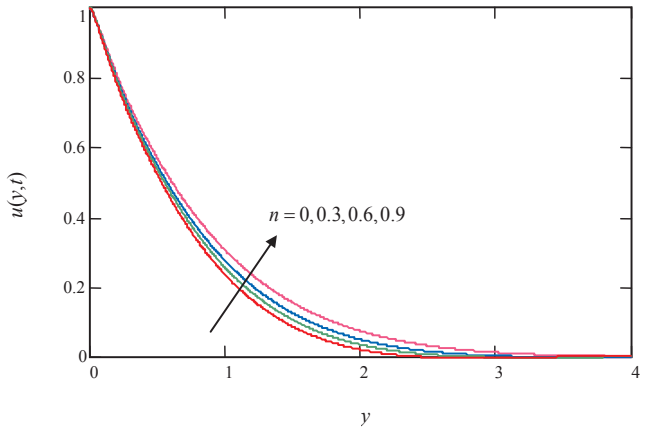

Fig. 6. Profiles of velocity for different values of n when $\beta = 0.5, \eta = 1.5, \Pr = 15, Gr = Gm = 5, M = K = 0.5, Sc = 0.2, \omega t = 0$ and $t = 0.6$.

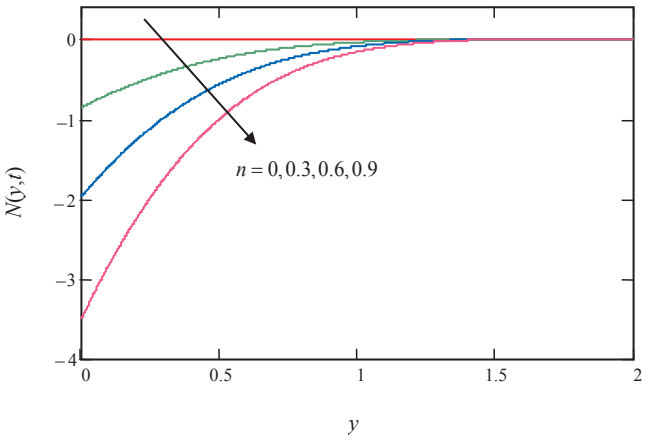

Fig. 7. Profiles of microrotations for different values of n when $\beta = 0.5, \eta = 1.5, \Pr = 15, Gr = Gm = 5, M = K = 0.5, Sc = 0.2, \omega t = 0$ and $t = 0.6$.

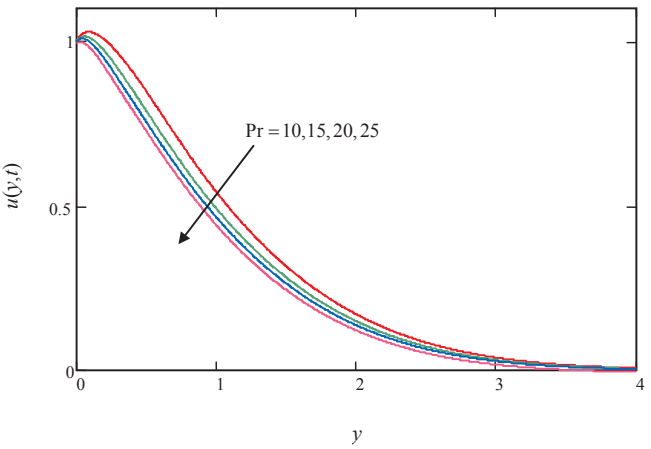

Fig. 8. Profiles of velocity for different values of Pr when $\beta = 0.5, \eta = 1.5, n = 0.6, Gr = Gm = 5, M = K = 0.5, Sc = 0.2, \omega t = 0$ and $t = 0.6$.

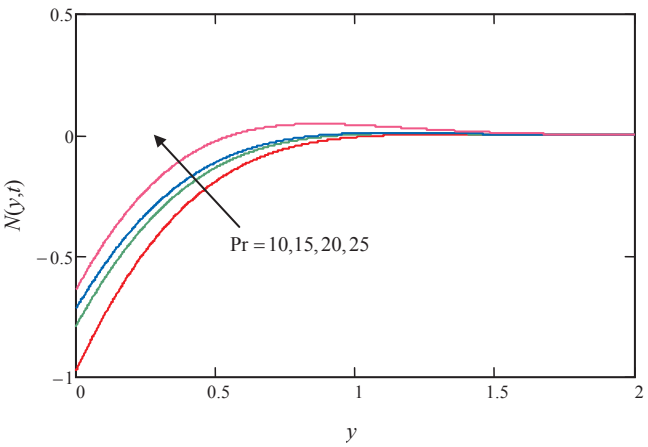

Fig. 9. Profiles of microrotations for different values of Pr when $\beta = 0.5, \eta = 1.5, n = 0.6, Gr = Gm = 5, M = K = 0.5, Sc = 0.2, \omega t = 0$ and $t = 0.6$.

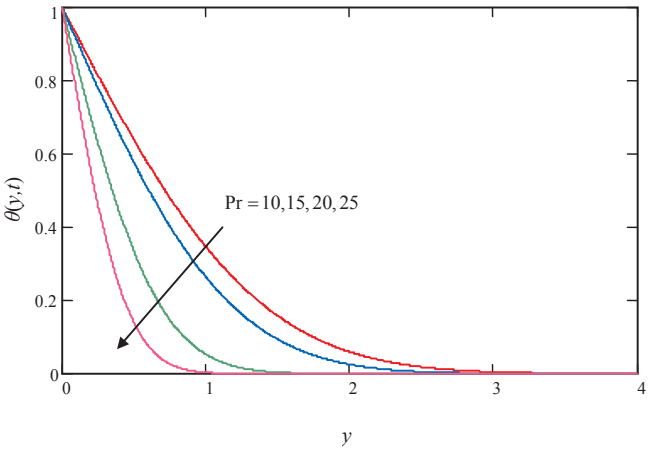

Fig. 10. Profiles of temperature for different values of Pr when $t = 0.4$.

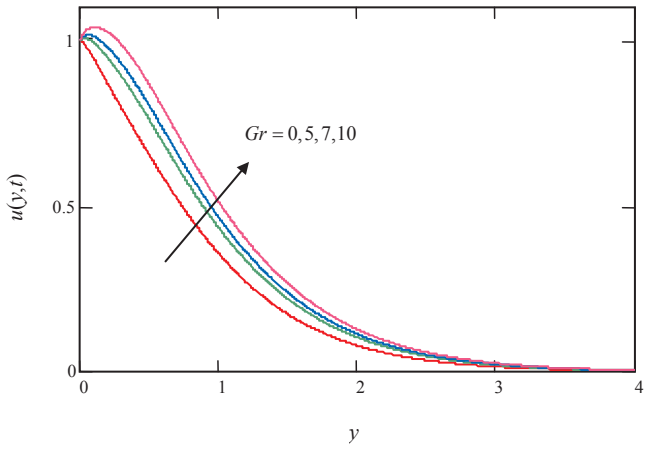

Fig. 11. Profiles of velocity for different values of Gr when $\beta = 0.5, \eta = 1.5, n = 0.6, \Pr = 15, Gm = 5, M = K = 0.5, Sc = 2, \omega t = 0$ and $t = 0.6$.

are shown in Figs. 17 and 18. It is seen that, velocity increases for increasing values of K. Physically, the existence of a porous medium in the flow presents resistance to flow. Thus, the resulting resistive force tends to slow the motion of the fluid along the plate surface and causes increases in its velocity profiles. On the other hand as K increases, the magnitude of the microrotation profiles tends to decrease.

The effect of Sc on velocity, microrotation and concentration profiles illustrated in Figs. 19–21, respectively. It is seen from these figures

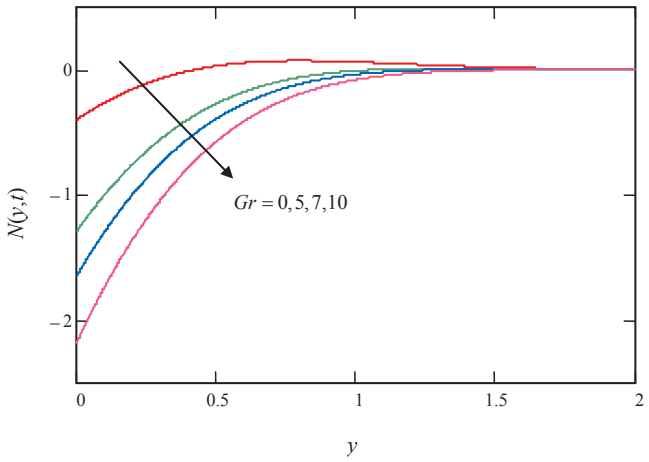

Fig. 12. Profiles of microrotations for different values of Gr when $\beta = 0.5, \eta = 1.5, n = 0.6, \mathrm{Pr} = 15, Gm = 5, M = K = 0.5, Sc = 2, \omega t = 0$ and $t = 0.6$.

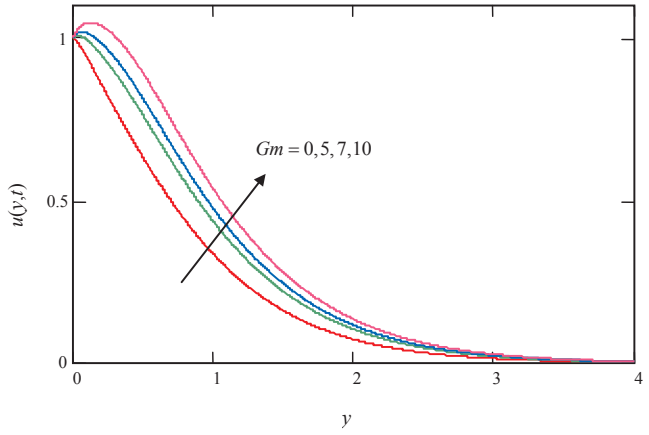

Fig. 13. Profiles of velocity for different values of Gm when $\beta = 0.5, \eta = 1.5, n = 0.6, \mathrm{Pr} = 15, Gr = 5, M = K = 0.5, Sc = 2, \omega t = 0$ and $t = 0.6$.

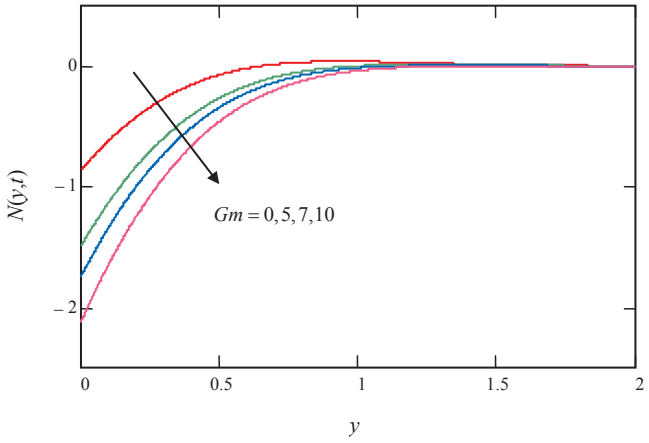

Fig. 14. Profiles of microrotations for different values of Gm when $\beta = 0.5, \eta = 1.5, n = 0.6, \mathrm{Pr} = 15, Gr = 5, M = K = 0.5, Sc = 2, \omega t = 0$ and $t = 0.6$.

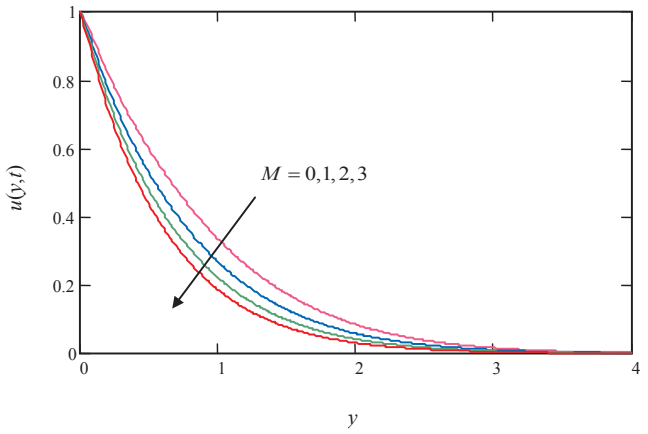

Fig. 15. Profiles of velocity for different values of M when

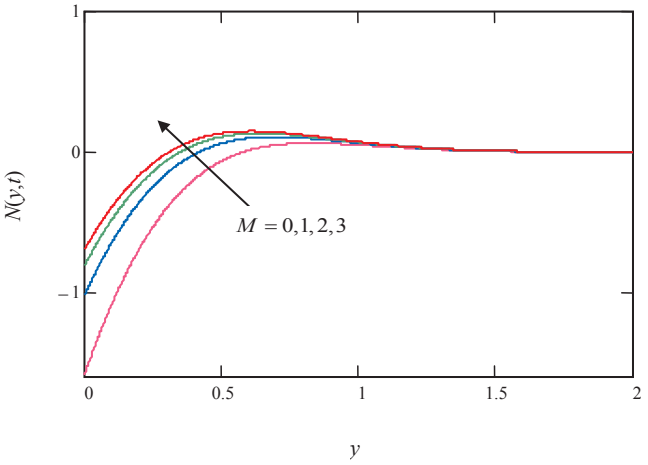

Fig. 16. Profiles of microrotations for different values of M when $\beta = 0.5, \eta = 1.5, n = 0.6, \mathrm{Pr} = 15, Gr = Gm = 5, K = 0.5, Sc = 0.2, \omega t = 0$ and $t = 0.6$.

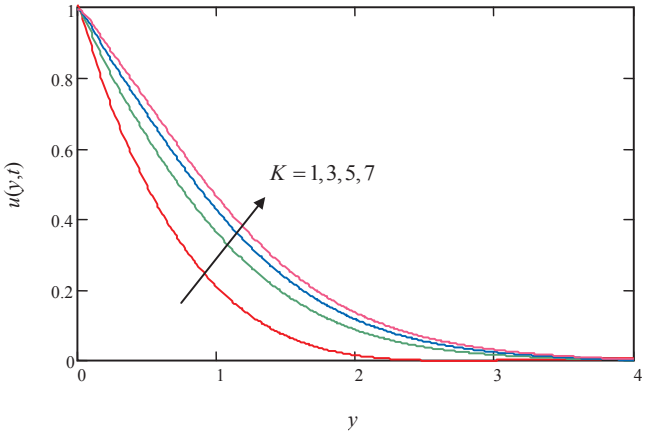

Fig. 17. Profiles of velocity for different values of K when $\beta = 0.5, \eta = 1.5, n = 0.6, \mathrm{Pr} = 15, Gr = Gm = 5, M = 0.5, Sc = 0.2, \omega t = 0$ and $t = 0.6$

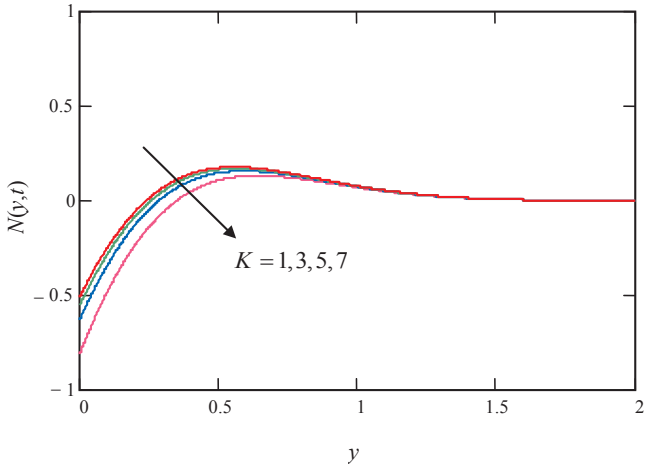

Fig. 18. Profiles of microrotations for different values of K when $\beta = 0.5, \eta = 1.5, n = 0.6, \Pr = 15, Gr = Gm = 5, M = 0.5, Sc = 0.2, \omega t = 0$ and $t = 0.6$

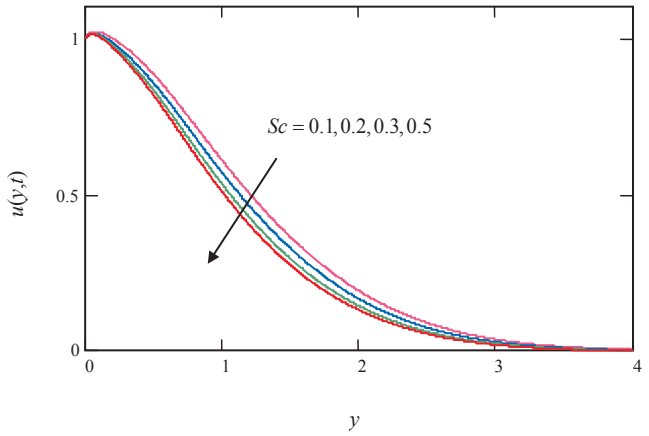

Fig. 19. Profiles of velocity for different values of Sc when $\beta = 0.5, \eta = 1.5, n = 0.6, \Pr = 15, Gr = Gm = 5, M = K = 0.5, \omega t = 0$ and $t = 0.6$.

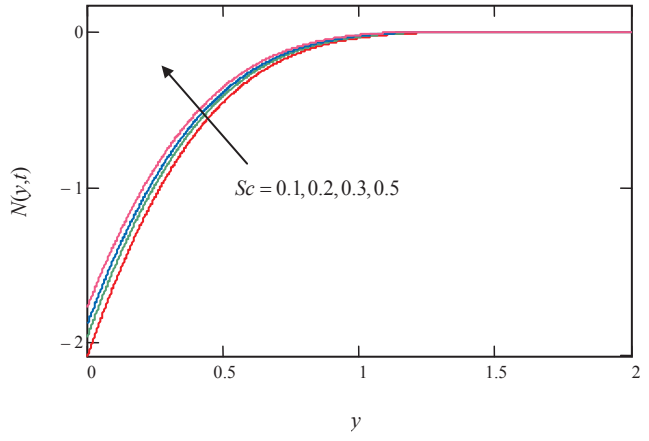

Fig. 20. Profiles of microrotations for different values of Sc when $\beta = 0.5, \eta = 1.5, n = 0.6, \Pr = 15, Gr = Gm = 5, M = K = 0.5, \omega t = 0$ and $t = 0.6$.

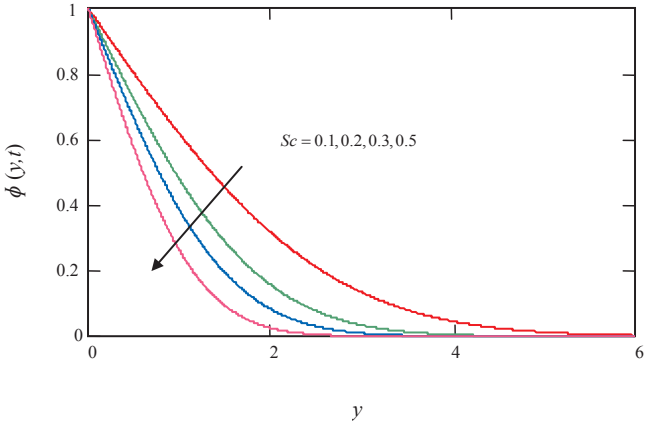

Fig. 21. Profiles of concentration for different values of Sc when $\Pr = 10$.

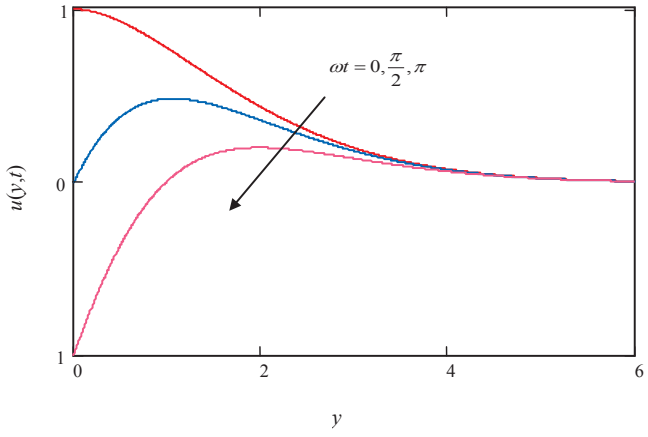

Fig. 22. Profiles of velocity for different values of ωt when $\beta = 0.5, \eta = 1.5, n = 0.6, \Pr = 15, Gr = Gm = 5, M = K = 0.5, Sc = 0.2$ and $t = 0.6$.

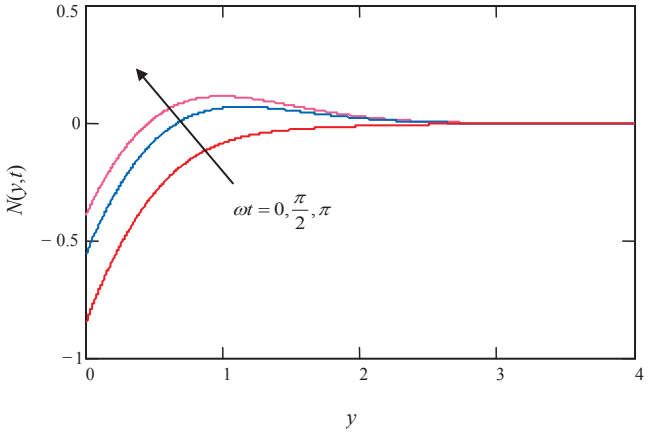

Fig. 23. Profiles of microrotations for different values of ωt when $\beta = 0.5, \eta = 1.5, n = 0.6, \Pr = 15, Gr = Gm = 5, M = K = 0.5, Sc = 0.2$ and $t = 0.6$.

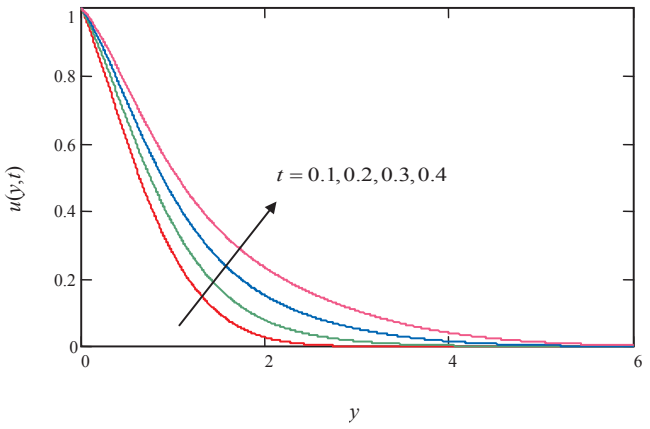

Fig. 24. Profiles of velocity for different values of t when

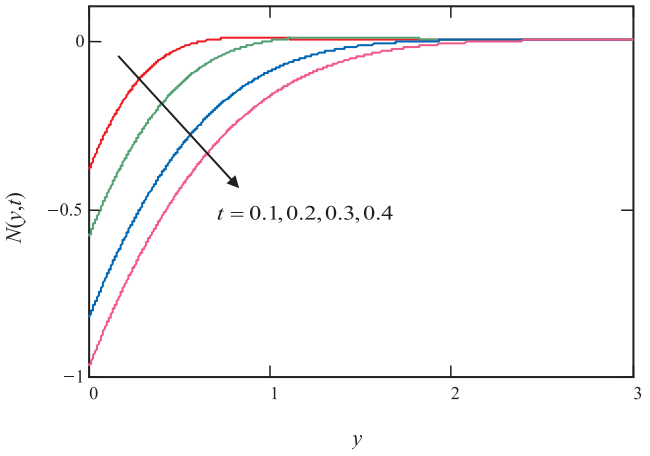

Fig. 25. Profiles of microrotations for different values of t when $\beta = 0.5, \eta = 1.5, n = 0.6, \mathrm{Pr} = 15, Gr = Gm = 5, M = K = 0.5$ and $Sc = 0.2$.

that with increasing Sc, velocity and concentration are tending to decrease across the boundary layer. Besides that Fig. 20 shows that the magnitude of microrotation increases as Sc increases. In Figs. 22 and 23 graphs are plotted for velocity and microrotation profiles for different values of ωt. It is found that the velocity presents an oscillatory behaviour. Instead, the magnitude of microrotation shows an increasing behaviour. Fig. 22 presents that velocity satisfies the imposed boundary condition (17). This figure can easily help us to check the accuracy of our results. Figs. 24 and 25 depict the effects of t on velocity and microrotation profiles. It is observed that velocity and microrotation have reverse relation with increasing values of t, whereas temperature increases with increasing t. In order to check the accuracy of present results, the velocity profiles of present result, Eq. (33) is compared with published results in literature Chaudhary and Jain [6]. This comparison is plotted in Fig. 26 and excellent agreement is observed.

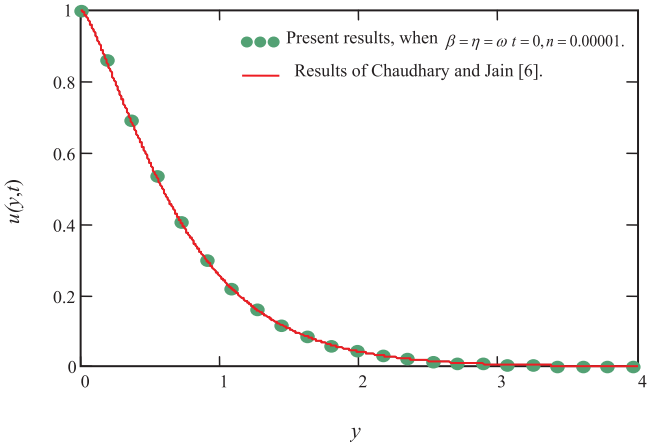

Fig. 26. Comparison of the present results (33), when $\beta = \eta = \omega t = 0$ and $n = 0.00001$ with results obtained by Chaudhary and Jain [6] see Eq. (19), when $\omega t = 0$ and $t = 0.6$.

Conclusion

In this study a combined phenomenon of heat and mass transfer in the MHD unsteady flow of an incompressible, homogeneous micropolar fluid past an oscillating vertical plate with isothermal temperate and constant mass diffusion in a porous medium has been investigated. The governing equations of the flow, together with initial and boundary conditions are written in the non-dimensional forms. The Laplace transforms and convolution technique used for closed forms solutions of the velocity, microrotation, temperature, and concentration have expressed in terms of exponential and complementary error functions. Based on the obtained solutions and using some graphical illustrations generated with the MATHCAD software, the following main points are concluded.

- Velocity across the boundary layer increases with increasing η, n, K, Gr, Gm and t whereas decreases with increasing values of $\beta, M, \mathrm{Pr}, Sc$ and ωt.
- Magnitude of microrotation on the plate is decreases with increasing η, n, K, Gr, Gm and t, while increases with increasing $\beta, M, \mathrm{Pr}, Sc$ and ωt.
- Temperature increases with increasing t, whereas concentration decreases with increasing Sc.
- The velocity is smaller for micropolar fluids than for Newtonian fluids.
- An excellent agreement of the present results (33) is found with existing results obtained by Chaudhary and Jain [6].

Conflict of interest

The authors have declared that no conflicts of interests exist.

Appendix A

$\Re_0 = \frac{1}{2} - nG_1 i\omega R_{14}$ $\Re_1 = \frac{1}{2} - nG_1 i\omega R_{13}$ $\Re_2 = \lambda_0 + \lambda_1$

$\Re_3 = \lambda_0 - nG_1 a_{11} R_9$ $\Re_4 = \lambda_1 - nG_1 a_{12} R_{10}$ $\Re_5 = \lambda_1 - nG_1 a_{12} R_{10}$

$\Re_6 = nG_1 \delta_3 R_{12}$ $\Re_7 = nG_1 \delta_3 A_2$ $\Re_8 = nG_1 a_{11} R_9$

$\Re_9 = nG_1 a_{12} R_{10}$ $\Re_{10} = i\omega n G_1 R_{13}$ $\Re_{11} = i\omega n G_1 R_{14}$

$\Re_{12} = nG_1 R_1 \sqrt{\beta_0}$ $\Re_{13} = nG_1 A_1 \sqrt{\beta_0}$ $\Re_{14} = nG_1 R_2 \sqrt{\beta_0}$

$\Re_{15} = nG_1 R_3 \sqrt{\beta_0}$ $\Re_{16} = nG_1 R_4 \sqrt{\beta_0}$ $\Re_{17} = nG_1 R_5 \sqrt{\beta_0}$

$\Re_{18} = nG_1 R_6 \sqrt{\beta_0}$ $\Re_{19} = nG_1 R_7 \sqrt{\beta_0}$ $R_1 = \frac{L_1}{\delta_3}$

$R_2 = \frac{L_2}{a_{11} - \delta_3}$ $R_3 = \frac{L_3}{a_{12} - \delta_3}$ $R_4 = \frac{L_4}{\delta_1 + \delta_3}$

$R_5 = \frac{L_5}{\delta_2 + \delta_3}$ $R_6 = \frac{L_6}{i\omega + \delta_3}$ $R_7 = \frac{L_7}{i\omega + \delta_3}$

$R_8 = \frac{L_8}{\delta_3}$ $R_9 = \frac{a_{11} L_9}{a_{11} - \delta_3}$ $R_{10} = \frac{a_{12} L_{10}}{a_{12} - \delta_3}$

$R_{11} = \frac{L_{11}}{\delta_1 + \delta_3}$ $R_{12} = \frac{L_{12}}{\delta_2 + \delta_3}$ $R_{13} = \frac{L_{13}}{i\omega + \delta_3}$

$R_{14} = \frac{L_{14}}{i\omega + \delta_3}$ $\lambda_0 = \frac{G_2}{a_{11}}$ $\lambda_1 = \frac{G_3}{a_{12}}$

$A_1 = R_1 - R_2 - R_3 + R_4 + R_5 - R_6 + R_7$ $A_2 = R_8 - R_9 - R_{10} + R_{11} + R_{12} - R_{13} + R_{14}$ $L_1 = -C_0 + C_1 - C_4 - \overline{C}_0 + \overline{C}_1 - \overline{C}_4$

$L_2 = C_0 - C_2 - C_5 - \overline{H}_7 + \overline{H}_8 + \overline{H}_9 - \overline{H}_{10}$ $L_3 = -\overline{C}_0 - \overline{C}_2 - \overline{C}_5 - \overline{H}_7 - \overline{H}_8 + \overline{H}_9 - \overline{H}_{10}$ $L_4 = -C_3 - \overline{C}_3 + H_7 - \overline{H}_7 - \overline{H}_9 + H_9 - l_3$

$L_5 = -C_6 - \overline{C}_6 - H_8 + H_{10} - \overline{H}_8 + \overline{H}_{10} + l_6$ $L_6 = l_0 - l_1 - l_4$ $L_7 = l_0 + l_2 + l_5$

$L_8 = -C_7 + C_{11} + C_{14} - C_{17} - \overline{C}_{17} - \overline{C}_7 + \overline{C}_{11} + \overline{C}_{14} - \overline{C}_{17}$ $L_9 = C_8 - C_{12} - C_{15} + C_{18} - H_0 + H_2 + H_5$ $L_{10} = \overline{C}_8 - \overline{C}_{12} - \overline{C}_{15} + \overline{C}_{18} - \overline{H}_0 + \overline{H}_2 + \overline{H}_5$

$+ H_0 - H_1 + H_4 + \overline{H}_4 + \overline{H}_0 - \overline{H}_1 - \overline{H}_4$

$L_{11} = C_9 - C_{16} + \overline{C}_9 - \overline{C}_{16} + H_3 - \overline{H}_3 - l_9 - l_{15}$ $L_{12} = -C_{13} + C_{19} - \overline{C}_{13} + \overline{C}_{19} + H_6 - \overline{H}_6 + l_{12} - l_{18}$ $L_{13} = l_7 - l_{10} - l_{13} + l_{16}$

$L_{14} = -l_8 + l_{11} + l_{14} - l_{17}$ $l_0 = \frac{W_0}{2}$ $l_1 = \frac{W_1}{2(i\omega + \delta_1)}$

$l_2 = \frac{W_1}{2(i\omega - \delta_1)}$ $l_3 = \frac{W_1 \delta_1}{2(\omega^2 - \delta_1^2)}$ $l_4 = \frac{W_2}{2(i\omega - \delta_2)}$

$l_5 = \frac{W_2}{2(i\omega - \delta_2)}$ $l_6 = \frac{W_1 \delta_2}{2(\omega^2 - \delta_2^2)}$ $l_7 = \frac{\beta_0 W_3(k_0 + i\omega)}{2i\omega(\delta_1 + i\omega)}$

$l_8 = \frac{\beta_0 W_3(-k_0 + i\omega)}{2i\omega(-\delta_1 + i\omega)}$ $l_9 = \frac{\beta_0 W_3(-k_0 + i\omega)}{2i\omega(-\delta_1^2 + \omega^2)}$ $l_{10} = \frac{\beta_0 W_3(k_0 + i\omega)}{2i\omega(\delta_2 + i\omega)}$

$l_{11} = \frac{\beta_0 W_3(-k_0 + i\omega)}{2i\omega(-\delta_2 + i\omega)}$ $l_{12} = \frac{\beta_0 W_3(-k_0 + i\omega)}{2i\omega(-\delta_2^2 + \omega^2)}$ $l_{13} = \frac{\beta_0 W_4(k_0 + i\omega)}{2i\omega(-\delta_1 + i\omega)}$

$l_{14} = \frac{\beta_0 W_4(-k_0 + i\omega)}{2i\omega(-\delta_1 + i\omega)}$ $l_{15} = \frac{\beta_0 W_4(-k_0 + i\omega)}{2i\omega(\delta_1^2 + \omega^2)}$ $l_{16} = \frac{\beta_0 W_4(-k_0 + i\omega)}{2i\omega(\delta_2 + i\omega)}$

$l_{17} = \frac{\beta_0 W_4(-k_0 + i\omega)}{2i\omega(-\delta_2 + i\omega)}$ $l_{18} = \frac{\beta_0 W_4(-k_0 + i\omega)}{2i\omega(-\delta_2^2 + \omega^2)}$ $H_0 = \frac{a_9 g_1 W_0}{a_{11}}$

$H_1 = \frac{a_9 g_1 W_1}{a_{11} \delta_1}$ $H_2 = \frac{a_9 g_1 W_1}{a_{11}(\delta_1 + a_{11})}$ $H_3 = \frac{a_9 g_1 W_1}{\delta_1(\delta_1 + a_{11})}$

$H_4 = \frac{a_9 g_1 W_2}{a_{11} \delta_2}$ $H_5 = \frac{a_9 g_1 W_2}{a_{11}(\delta_2 + a_{11})}$ $H_6 = \frac{a_9 g_1 W_2}{\delta_2(\delta_2 + a_{11})}$

$H_7 = \frac{a_9 g_1 W_3}{\delta_1 + a_{11}}$ $H_8 = \frac{a_9 g_1 W_3}{\delta_2 + a_{11}}$ $H_9 = \frac{a_9 g_1 W_4}{\delta_1 + a_{11}}$

$H_{10} = \frac{a_9 g_1 W_4}{\delta_2 + a_{11}}$ $\overline{H}_0 = \frac{a_9 g_2 W_0}{a_{12}}$ $\overline{H}_1 = \frac{a_9 g_2 W_1}{a_{12} \delta_1}$

$\overline{H}_2 = \frac{a_9 g_2 W_1}{a_{12}(\delta_1 + a_{12})}$ $\overline{H}_3 = \frac{a_9 g_2 W_1}{\delta_1(\delta_1 + a_{12})}$ $\overline{H}_4 = \frac{a_9 g_2 W_2}{a_{12} \delta_1}$

$\overline{H}_5 = \frac{a_9 g_2 W_2}{a_{12}(\delta_2 + a_{12})}$ $\overline{H}_6 = \frac{a_9 g_2 W_2}{\delta_2(\delta_2 + a_{12})}$ $\overline{H}_7 = \frac{a_9 g_2 W_3}{\delta_1 + a_{12}}$

$\overline{H}_8 = \frac{a_9 g_2 W_3}{\delta_2 + a_{12}}$ $\overline{H}_9 = \frac{a_9 g_2 W_4}{\delta_1 + a_{12}}$ $\overline{H}_{10} = \frac{a_9 g_2 W_4}{\delta_2 + a_{12}}$

$C_0 = \frac{g_1 W_1}{a_{11}}$ $C_1 = \frac{g_1 W_1}{a_{11} \delta_1}$ $C_2 = \frac{g_1 W_1}{a_{11}(\delta_1 + a_{11})}$

$C_3 = \frac{g_1 W_1}{\delta_1(\delta_1 + a_{11})}$ $C_4 = \frac{g_1 W_2}{a_{11} \delta_2}$ $C_5 = \frac{g_1 W_2}{a_{11}(\delta_2 + a_{11})}$

$C_6 = \frac{g_1 W_2}{\delta_2(\delta_2 + a_{11})}$ $C_7 = \frac{\beta_0 g_1 W_3 k_0}{a_{11} \delta_2}$ $C_8 = \frac{\beta_0 g_1 W_3(a_{11} + k_0)}{a_{11}(\delta_1 + a_{11})}$

$C_9 = \frac{\beta_0 g_1 W_3(k_0 - \delta_1)}{\delta_1(\delta_1 + a_{11})}$ $C_{11} = \frac{\beta_0 g_1 W_3 k_0}{a_{11} \delta_2}$ $C_{12} = \frac{\beta_0 g_1 W_3(a_{11} + k_0)}{a_{11}(\delta_2 + a_{11})}$

$C_{13} = \frac{\beta_0 g_1 W_3(k_0 - \delta_2)}{\delta_2(\delta_2 + a_{11})}$ $C_{14} = \frac{\beta_0 g_1 W_4 k_0}{a_{11} \delta_1}$ $C_{15} = \frac{\beta_0 g_1 W_4(a_{11} + k_0)}{a_{11}(\delta_1 + a_{11})}$

$C_{16} = \frac{\beta_0 g_1 W_4(k_0 - \delta_1)}{\delta_1(\delta_1 + a_{11})}$ $C_{17} = \frac{\beta_0 g_1 W_4 k_0}{a_{11} \delta_2}$ $C_{18} = \frac{\beta_0 g_1 W_4(a_{11} + k_0)}{a_{11}(\delta_2 + a_{11})}$

$C_{19} = \frac{\beta_0 g_1 W_4(k_0 - \delta_2)}{\delta_2(\delta_2 + a_{11})}$ $\overline{C}_0 = \frac{g_2 W_1}{a_{12}}$ $\overline{C}_1 = \frac{g_2 W_1}{a_{11} \delta_1}$

$\overline{C}_2 = \frac{g_2 W_1}{a_{12}(\delta_1 + a_{12})}$ $\overline{C}_3 = \frac{g_2 W_1}{\delta_1(\delta_1 + a_{12})}$ $\overline{C}_4 = \frac{g_2 W_1}{a_{12} \delta_1}$

$\overline{C}_5 = \frac{g_2 W_2}{a_{12}(\delta_2 + a_{12})}$ $\overline{C}_6 = \frac{g_2 W_2}{\delta_2(\delta_2 + a_{12})}$ $\overline{C}_7 = \frac{\beta_0 g_2 W_2 k_0}{a_{12} \delta_1}$

$\overline{C}_8 = \frac{\beta_0 g_2 W_2(a_{12} + k_0)}{a_{12}(\delta_1 + a_{12})}$ $\overline{C}_9 = \frac{\beta_0 g_2 W_3(k_0 - \delta_1)}{\delta_1(\delta_1 + a_{12})}$ $\overline{C}_{11} = \frac{\beta_0 g_2 W_3 k_0}{a_{12} \delta_2}$

$$\overline{C}_{12} = \frac{\beta_0 g_2 W_3(a_{12}+k_0)}{a_{12}(\delta_2+a_{12})} \quad \overline{C}_{13} = \frac{\beta_0 g_2 W_3(k_0-\delta_2)}{\delta_2(\delta_2+a_{12})} \quad \overline{C}_{14} = \frac{\beta_0 g_2 W_4 k_0}{a_{12}\delta_1}$$

$$\overline{C}_{15} = \frac{\beta_0 g_2 W_4(a_{12}+k_0)}{a_{12}(\delta_1+a_{12})} \quad \overline{C}_{16} = \frac{\beta_0 g_2 W_4(k_0-\delta_1)}{\delta_1(\delta_1+a_{12})} \quad \overline{C}_{17} = \frac{\beta_0 g_2 W_4 k_0}{a_{12}\delta_2}$$

$$\overline{C}_{18} = \frac{\beta_0 g_2 W_4(a_{12}+k_0)}{a_{12}(\delta_2+a_{12})} \quad \overline{C}_{19} = \frac{\beta_0 g_2 W_4(k_0-\delta_2)}{\delta_2(\delta_2+a_{12})} \quad W_0 = 1-d_8$$

$$W_1 = \frac{d_9\delta_1 - d_8\delta_1^2}{\delta_1-\delta_2} \quad W_2 = \frac{d_9\delta_2 - d_8\delta_2^2}{\delta_1-\delta_2} \quad W_3 = \frac{d_6}{\delta_1-\delta_2}$$

$$W_4 = \frac{d_7}{\delta_1-\delta_2} \quad d_1 = a_2 - a_8 \quad d_2 = d_1^2 + a_1^2\beta_0 n^2$$

$$d_3 = 2a_3 d_1 + a_1^2\beta_0 n^2 k_0 \quad d_4 = a_2 d_1 - d_1^2 + a_1^2\beta_0 n^2 k_0 \quad d_5 = -a_2 a_3 + a_3 d_1 + a_1^2\beta_0 n^2 L$$

$$d_6 = \frac{a_1 a_3 n}{d_2} \quad d_7 = \frac{a_1 a_2 n}{d_2} \quad d_8 = \frac{d_1}{d_2}$$

$$d_9 = \frac{d_5}{d_2} \quad \delta_1 = \frac{m_2}{2} - \sqrt{\frac{m_2^2 - 4m_1 a_3}{2}} \quad \delta_2 = \frac{m_2}{2} + \sqrt{\frac{m_2^2 - 4m_1 a_3}{2}}$$

$$\delta_3 = \frac{a_3}{a_2} \quad G_1 = \frac{a_1}{a_2} \quad G_2 = Gr\frac{\beta_0}{a_5}$$

$$G_3 = Gm\frac{\beta_0}{a_7} \quad m_1 = \frac{a_3}{a_2} \quad m_2 = \frac{d_3}{d_2}$$

$$m_3 = \frac{d_1}{d_2} \quad g_1 = \frac{a_4}{a_5} \quad g_2 = \frac{a_6}{a_7}$$

$$a_{11} = \frac{a_3}{a_5} \quad a_{12} = \frac{a_3}{a_7} \quad a_1 = \beta\beta_0\sqrt{\eta}$$

$$a_2 = \eta - \beta_0 \quad a_3 = \beta_0 k_0 \quad a_4 = \beta_0 Gr$$

$$a_5 = \mathrm{Pr} - \beta_0 \quad a_6 = \beta_0 Gm \quad a_7 = Sc - \beta_0$$

$$a_8 = n\beta\beta_0\eta \quad a_9 = n\sqrt{\mathrm{Pr}} \quad a_{10} = n\sqrt{Sc}$$

$$k_0 = M + \frac{1}{K} \quad \beta_0 = \frac{1}{1+\beta}$$

References

[1] Eringen AC. Theory of micropolar fluids. J Math Mech 1966;16:1–18.
[2] Eringen AC. Theory of thermomicropolar fluids. J Math Anal Appl 1972;38:480–96.
[3] Eringen AC. Microcontinuum field theories II: fluent media. New York: Springer; 2001.
[4] Lukaszewicz G. Micropolar fluids: theory and applications. Basel: Birkhauser; 1999.
[5] Khan A, Khan I, Ali F, Khalid A, Shafie S. Exact solutions of heat and mass transfer with MHD flow in a porous medium under time dependent shear stress and temperature. Abstr Appl Aanl 2015;2015. org/10.1155/2015/975201.
[6] Chaudhary RC, Jain A. Combined heat and mass transfer effects on MHD free convection flow past an oscillating plate embedded in porous medium. Rom J Phys 2007;52:505–24.
[7] Senapati N, Dhal RK, Das TK. Effects of chemical reactions on free convection MHD flow through porous medium bounded by vertical surface with slip flow region. Am J Comput Appl Math 2012;2:124–35.
[8] Kim YJ. Unsteady MHD convection flow of polar fluids past a vertical moving porous plate in a porous medium. Int J Heat Mass Transfer 2001;44:2791–9.
[9] Harada N, Tsunoda K. Study of a disk MHD generator for nonequilibrium plasma generator (NPG) system. Energy Convers Manage 1998;39:493–503.
[10] Kirillov IR, Reed CB, Barleon L, Miyazaki K. Present understanding of MHD and heat transfer phenomena for liquid metal blankets. Fusion Eng Des 1995;27:553–69.
[11] Shang JS. Recent research in magneto-aerodynamics. Prog Aerosp Sci 2001;37:1–20.
[12] Abricka M, Krüminš J, Gelfgat Yu. Numerical simulation of MHD rotator action on hydrodynamics and heat transport in single crystal growth processes. J Cryst Growth 1997;180:388–400.
[13] Kim YJ. Unsteady convection flow of micropolar fluids past a vertical porous moving plate with variable suction. Acta Mech 2001;148:106.
[14] Ibrahim FS, Hassanien IA, Bakr AA. Unsteady MHD micropolar fluid flow and heat transfer over a vertical porous medium in the presence of thermal and mass diffusion with constant heat source. Can J of Phys 2004;82:775.
[15] Mohamed RA, Abo-Dahab SM. Influence of chemical reaction and thermal radiation on the heat and mass transfer in MHD micropolar flow over a vertical moving porous plate in a porous medium with heat generation. Int J Therm Sci 2009;48:800–1813.
[16] Hiremath PS, Patil PM. Free convection effects on the oscillatory flow of a couple stress fluid through a porous medium. Acta Mech 1993;98:143.
[17] Khalid A, Khan I, Shafie S. Heat transfer in ferrofluid with cylindrical shape nanoparticles past a vertical plate with ramped wall temperature embedded in a porous medium. J Mol Liq 2016;221:1175–83.
[18] Aurangzaib Kasim ARM, Mohammad NF, Sharidan S. Unsteady MHD mixed convection flow with heat and mass transfer over a vertical plate in a micropolar fluid-saturated porous medium. J Appl Sci Eng 2012;16:141–50.
[19] Modatheri M, Rashadi AM, Chamkha AJ. An analytical study of MHD heat and mass transfer oscillatory flow of a micropolar fluid over a vertical permeable plate in a porous medium. Turkish J Eng Env Sci 2009;33. 245 25.
[20] Mahmoud Mostafa AA, Waheed Shimaa E. MHD flow and heat transfer of a micropolar fluid over a stretching surface with heat generation (absorption) and slip velocity. J Egypt Math Soc 2012;20:20–7.
[21] Zia ul Haque Md, Mahmud Alam Md, Ferdows M, Postelnicu A. Micropolar fluid behaviors on steady MHD free convection and mass transfer flow with constant heat and mass fluxes, joule heating and viscous dissipation. J King Saud Univ Eng Sci 2012;24:71–84.
[22] Abo-Dahab SM, Mohamed RA. Unsteady flow of rotating and chemically reacting MHD micropolar fluid in slip-flow regime with heat generation. Int J Thermophys 2013;34:2183–208.
[23] Sajjad H, Farooq A. Effects of heat source/sink on MHD flow of micropolar fluids over a shrinking sheet with mass suction. J Basic Appl Sci Res 2014;4:207–15.
[24] Mishra SR, Dash GC, Pattnaik PK. Flow of heat and mass transfer on MHD free convection in a micropolar fluid with heat source. Alexandria Eng J 2015;54:3.
[25] Nadeem S, Hussain M. Naz M (2010) MHD stagnation flow of a micropolar fluid through a porous medium. Meccanica 2010;45:869–80.
[26] Agarwal RS, Dhanapal C. Flow and heat transfer in a micropolar fluid past a flat plate with suction and heat sources. Int J Eng Sci 1988;26:1257–66.
[27] Srinivasacharya D, Rajyalakshmi I. Creeping flow of a micropolar fluid past a porous sphere. Appl Math Comput 2004;153:843–54.
[28] Abo-Eldahab EM, Ghonaim AF. Radiation effect on heat transfer of a micropolar fluid through a porous medium. Appl Math Comput 2005;169:500–10.
[29] Damseh RA, Al-Azab TA, Shannak BA, Husein MA. Unsteady natural convection heat transfer of micropolar fluid over a vertical surface with constant heat flux. Turkish J Eng Env Sci 2007;31:225–33.
[30] Sheikholeslami M, Ashorynejad HR, Ganji DD, Rashidi MM. Heat and mass transfer of a micropolar fluid in a porous channel. Comm Num Anal 2014;2014:1–20.
[31] Hussanan A, Salleh MZ, Khan I, Tahar RM. Unsteady free convection flow of a micropolar fluid with Newtonian heating: Closed form solution. Therm Sci 2015. 125–125.
[32] Bakr AA, Raizah ZAS, Elaiw MA. MHD micropolar fluid near a vertical plate with Newtonian heating and thermal radiation in the presence of mass diffusion. Pure Appl Math J 2015;4:80–9.
[33] Khalid A, Khan I, Khan A, Shafie S. Conjugate transfer of heat and mass in unsteady flow of a micropolar fluid with wall couple stress. AIP Adv 2015;5:127125.
[34] Mohanty B, Mishra SR, Pattanayak HB. Numerical investigation on heat and mass transfer effect of micropolar fluid over a stretching sheet through porous media. Alexandria Eng J 2015;54:223–32.
[35] Pal D, Biswas S. Perturbation analysis of magnetohydrodynamics oscillatory flow on convective-radiative heat and mass transfer of micropolar fluid in a porous medium with chemical reaction. Eng Sci Tech Int J 2016;19:444–62.
[36] Hetnarski RB. On inverting the Laplace transforms connected with the error function. Appl Math 1964;7:1233–7234.
[37] Pal D, Rudraiah N, Devanathan R. A couple stress model of blood flow in the microcirculation, Bull. Math. Biol. 50: 329–344Ramanaiah G (1979) Squeeze films between finite plates lubricated by fluids with couple stresses. Wear 1988;17:315–20.
[38] Mokhiamar UM, Crosby WA, EL-Gamel HA. A study of journal bearing lubricated by fluids with couple stresses considering the elasticity of the liner. Wear 1999;224:194–201.
[39] Zakaria M. MHD unsteady free convection flow of a couple stress fluid with one relaxation time through a porous medium. Appl Math Comput 2003;146:469–94.
[40] Sreenadh S, Kishore SN, Srinivas ANS, Reddy RH. MHD Free convection flow of

couple stress in a vertical porous layer. Adv Appl Sci Res 2011;2(6):215–22.
[41] Khan NA, Riaz F. Off-centered stagnation point flow of a couple stress fluid towards a rotating disk. Sci World J 2014:163586.
[42] Rani HP, Reddy GJ, Kim CN. Couple stress fluid over an infinite vertical cylinder. Eng Appl Comput Fluid Mech 2011;5:159–69.
[43] Srinivasacharya D, Kaladhar K. Analytical solution for Hall and ion-slip effects on couple stress fluid between the parallel disks. Math Comput Model 2013;57:2494–509.
[44] El-Dabe NTM, El-Mohandis SMG. Effect of couple stresses on pulsatile hydro-magnetic Poiseuille flow. Fluid Dyn Res 1995;15:313–24.
[45] Farooq M, Islam S, Rahim MT, Siddiqui AM. Laminar flow of couple stress fluids for Vogel's model. Sci Res Essays 2012;7(33):2936–61.
[46] Khan NA, Mahmood A, Ara A. Approximate solution of couple stress fluid with expanding or contracting porous channel. Eng Comput 2012;30(3):399–408.